Scanning force microscopy experiments probing micromechanical properties on polymer surfaces using harmonically modulated friction techniques II. Investigations of heterogeneous systems

Heinz Sturm, Eckhard Schulz*, Martin Munz

Department "Performance of Polymer Materials"
Federal Institute for Materials Research and Testing (BAM)
Unter den Eichen 87, D-12205 Berlin, Germany

SUMMARY: Applying a high-frequency lateral vibration between tip and sample in a scanning force microscope (SFM), a harmonically modulated lateral (friction) force image can be obtained using lock-in techniques. Harmonically modulated lateral force microscopy (HM-LFM) offers several advantages compared with standard lateral force microscopy (LFM). After a brief investigation of the scan velocity dependence of LFM and HM-LFM, two samples were investigated. First, the surface of a poly(acrylonitrile-*co*-styrene)/polybutadiene blend (ABS) was used to demonstrate the ability of the new technique to decrease the stick effects of the SFM tip. Second, an interface between two chemically very similar polymers was prepared by melting polypropylene (PP) and poly(propene-*block*-ethene) (PP-*block*-PE) films on each other. After cutting, the surface roughness of this sample was very high. It is shown that only HM-LFM clearly resolves the local micromechanical properties without artefacts.

Introduction

In scanning force microscopy (SFM), the lateral force between the tip and the sample surface leads to torsion of the tip carrying cantilever during the scanning process[1]. Analysing the reflected light from the cantilever beam, this torsion can be measured and can be visualised as an image, which is interpreted as a contrast of local friction processes (lateral force microscopy, LFM)[2]. However, the cross-talk of the topography, i.e., the edge-correlated friction makes it difficult or sometimes even impossible to determine local friction contrasts, which belong to different micromechanical material properties. In contrast to LFM, the method we use implements a small high-frequency lateral vibrational movement between the tip and sample surface. The amplitude and the phase shift of the harmonically modulated cantilever torsion can be extracted from the photodiode signal using lock-in techniques[3]. After the build-up of the instrument and some performance tests (see Part I, this journal), we focus our interest on the influence of the scan velocity. As mentioned in Part I, low scan speeds increase the risk of sticking and so the chance of surface destruction. On the other hand, there are advantages of an optimised feedback and a larger torsion angle of the lever,

 CCC 1022-1360/99/$ 17.50+.50/0

both increasing the sensitivity and trueness of the topography and the HM-LFM signal. A first investigation should show the main dependences to roughly verify these predictions.

The influence of topography on LFM images

Several artefacts of LFM often hinder a deeper understanding of the material-dependent friction processes. One reason is that the constant-force feedback never works with absolute precision, because creep and hysteresis of the piezoelectric transducers occur and the bandwidth of the electronics is limited.

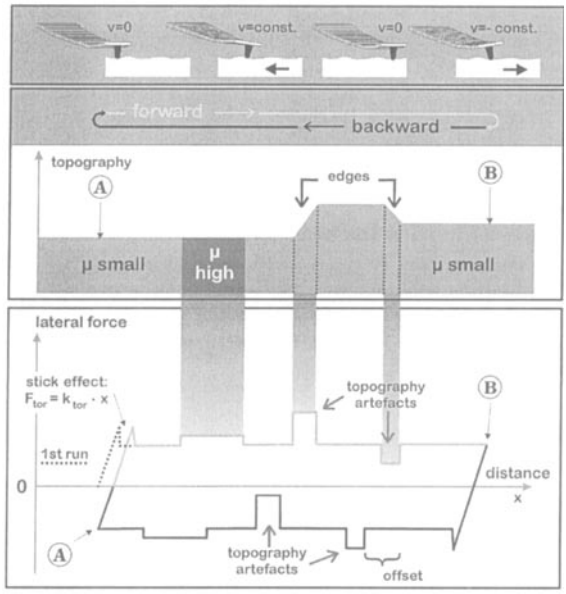

Fig. 1: True and artificial LFM contrasts and the influence of the stick-slip effect

As shown in Fig. 1, artefacts will occur in the friction force traces at topography steps. Hence, on a rough sample surface, a subtraction of the forward (A-B) and backward (B-A) trace is necessary to evaluate a contrast of the friction coefficient μ. However, the distance offset between the forward and backward scan traces caused after the reversal of the lever torsion (stick effect) needs compensation. Flat surfaces, on the other hand, often cause problems due to an interference of the laser light reflected from the cantilever beam and the sample. The interference-induced intensity modulation can disturb the topography and the lateral force signals independently. Often only one of them can be desensitized by adjustment of the angles between the sample surface and the photodiode. For image sizes in the micrometer range, about a dozen of stripe-like intensity modulations artefacts can occur caused by the interference phenomenon (see Fig. 8b). Using the HM-LFM technique, the demodulated high-frequency lateral force signal should not depend on this intensity modulation. Additionally, the low-frequency torsion of the lever (i.e., the edge-induced cross-talk of the topography) should not affect the HM-LFM image either.

Sample preparation and characterisation

A set of samples with heterogeneous surface properties was prepared as follows. A dilute solution of poly(acrylonitrile-*co*-styrene)/polybutadiene blend (ABS) in tetrahydrofuran gives a thin film with small, flat holes of the phase-segregated polymers. The holes are a consequence of the low polymer concentration. The substrate is a gold film (ca. 50 nm) sputtered on a silicon wafer (sample A, reference sample) or a flat ABS surface of an injection-moulded part (sample B, investigated with HM-LFM).

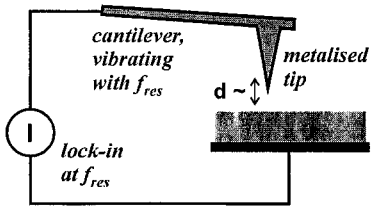

Fig. 2: Schematic diagram of the signal pathway in the non-contact-mode SFM for imaging of surface charges by electrostatic induction

The reference sample was characterised by surface charge microscopy[4] using a non-contact SFM with a metalised and grounded tip (Fig. 2), the lever resonance frequency f_{res} being ~75 kHz. Electrostatic induction in the tip, which depends on the amount of the surface charge and the tip-to-sample distance, gives an AC current which is measured by a synchronised lock-in amplifier. Under constant distance conditions of the tip and surface, the AC current reflects the amount of charge and potential. The contrast mechanism depends on the work function (Fermi level), the local permittivity and the conductivity as well. The topography is measured simultaneously. A typical height of the steps in Fig. 3a is 90-100 nm. Within the holes formed by the dewetting process, a film thickness of several nanometers is reasonable. The imaginary part of the charge-induced displacement current, given in Fig. 3b, is attributed to dissipation

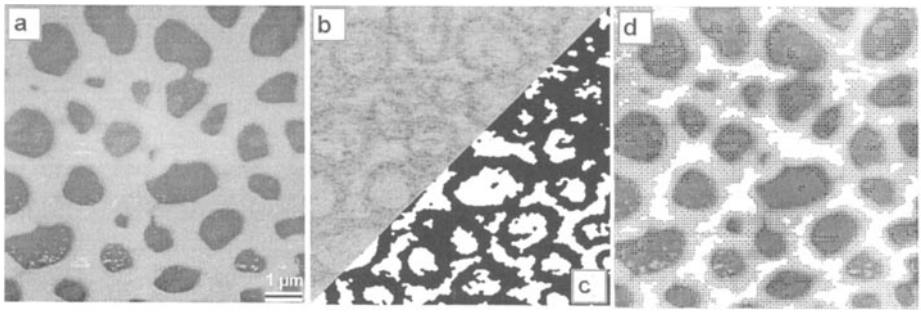

Fig. 3: ABS film, dewetted from THF on a gold substrate (reference sample, A). Scan speed 6 µm/s (non-contact-mode SFM). (a) Topography contrast, corrugation 172 nm; (b) surface charge contrast [a.u.]; (c) surface charge contrast, two-bit colour representation; (d) superposition of the topography and the two-bit image (crosshatched) of the surface charge, showing the heterogeneity of the "bridges" and "grooves"

processes of charge carriers and dipoles. The surface charge distribution is reduced to a two-bit image (Fig. 3c). Dark areas belong to polybutadiene, whereas the bright sections are poly(acrylonitrile-*co*-styrene). This composition analysis is confirmed by measurements of local mechanical properties. Superimposing the two-bit image to the topography (Fig. 3d), the result of the dewetting process is obvious: polybutadiene typically prefers to form the edges of the holes and grooves.

The second sample consists of an interface zone between two polymers which was prepared by melting PP and PP-*block*-PE films on each other. This sample was cut perpendicular to the films plane with a steel knife (sample C). Consequently, its surface is very rough.

The preparation of a thin film of poly(styrene-*block*-methyl methacrylate) (PS-*block*-PMMA, sample D) from a dilute toluene solution is described elsewhere[5].

Results and Discussion

Figure 4 shows the surface of an ABS hole film dewetted on an ABS substrate, the depth of the holes being between 50 and 250 nm. This image corresponds to the schematic drawing of the image field in Fig. 5a, where the relation between the image field and overscan region is demonstrated.

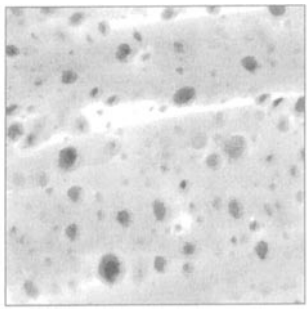

Fig. 4: Surface of reference sample B, image size 10x10 µm, scan speed 7 µm/s

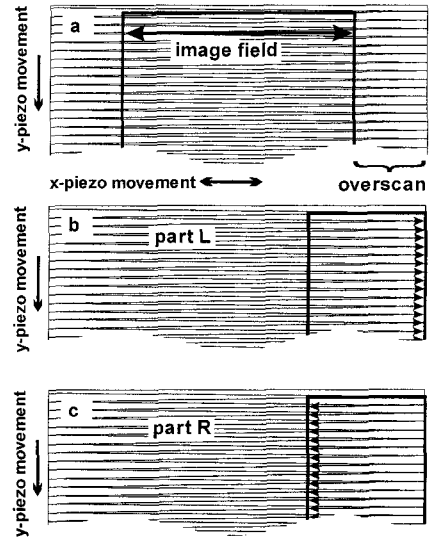

Fig. 5: (a) Image field not manipulated, overscan is used to prevent problems with lever vibration. After manipulation: (b) left part L is scanned from left to the right, (c) right part R is scanned from right to the left (see Fig. 7)

In SFM, the overscan is useful to reduce the noise which is induced by the ringing of the cantilever after it changes the scanning direction. After manipulation of the synchronisation procedure between the scanner movement and the digitising of the data, it is possible to observe micromechanical properties (LFM and HM-LFM) with different scan speeds and directions in the overscan region.

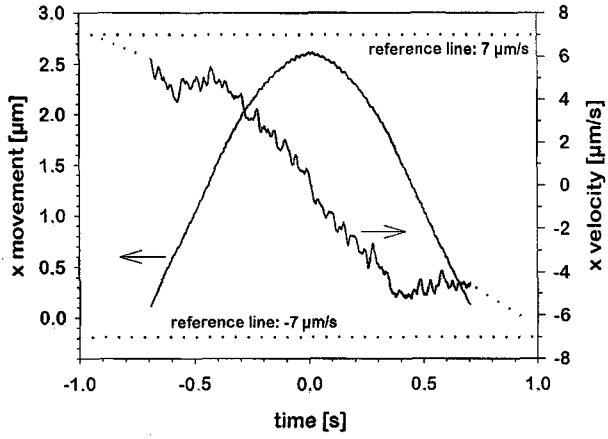

Fig. 6: Movement of x-piezo and tip velocity in the overscan region used in Fig. 7 vs. time

Figure 6 shows the movement of the x-piezo and the velocity of the tip in the overscan region. The tip velocity changes discontinuously, the reference lines give the scan speed during the conventional imaging (Fig. 4).

Figure 7a gives an image of the local normal force. Most features appear twice, the image has a vertical mirror axis. At the edge of a hole, the tip has to decline but the constant force feedback is not perfectly fast: for a short time, the normal force is lower than it should be (i.e., darker). After the flat hole is crossed, the normal force is slightly higher than it should be (brighter) for the same reasons. At the same edge during the back scan (part R), these effects are present but inverse (see Fig. 1).

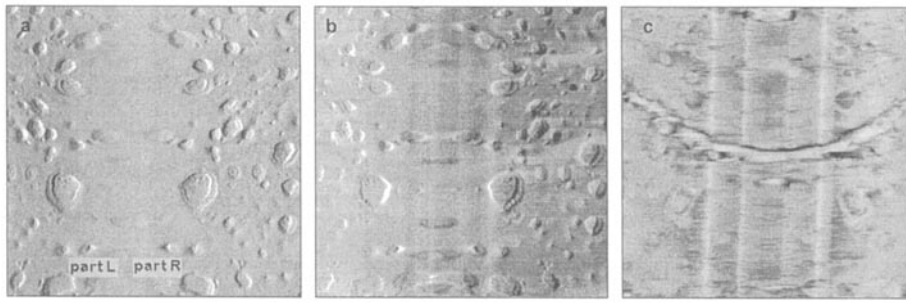

Fig. 7: Images of (a) the normal force, (b) the lateral force and (c) the harmonically modulated lateral force (vertical size 10 µm, grey scale in a.u.) in sample B. Due to a high sensitivity to the tip velocity, vertical stripes occur mainly in (c) during the discontinuous changes of the scanning speed (see Fig. 6)

Figure 7b shows the LFM image. At the edges of the holes, the presence of polybutadiene should lead to a clear micromechanical friction contrast. However, edge-correlated friction makes it impossible to interpret or recalculate the data.

Figure 7c gives the HM-LFM signal. It can be noticed that several holes are surrounded by bright rings, i.e., a higher high-frequency friction signal, which is expected for the soft polybutadiene phase. It does not depend on the scanning direction. A second fact can be evaluated from these images. For a short time of several milliseconds, the scanning velocity is small enough to enable the tip sticking at the polymer surface. However, an advantageous micromechanical behaviour can be observed. Due to the additional lateral vibration during the measurement, a stick-slip behaviour and the thus induced ringing of the cantilever is avoided.

The next presented experiment shows that HM-LFM is a superior method especially for ill-prepared sample surfaces. Precision and reliability of surface composition investigations with SFM often suffers from the fact that the surface quality is bad and that the surface roughness is very high.

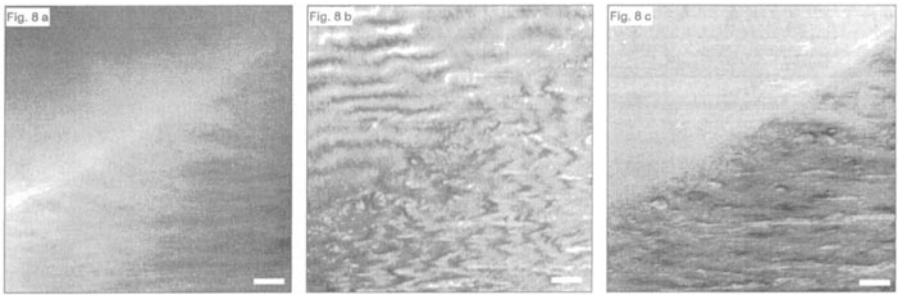

Fig. 8: (a) Topography of sample C (image size 28x28 μm, bar 3 μm, Δz range 2514 nm, scan speed 50 μm/s, normal load $F_N \approx 15$ nN, measured in air at 20 °C); (b) conventional lateral force image (LFM) measured simultaneously; (c) harmonically modulated LFM image measured simultaneously (lateral vibration < 31 nm, vibration frequency 44 kHz, PP: bright, PP-*block*-PE: dark)

Figure 8a gives the surface topography at the interface between PP and PP-*block*-PE. The cutting with a steel knife at room temperature leads to a very rough sample surface. The LFM contrast given in Fig. 8b is very noisy and dominated by a well-known artefact: the reflected laser light from the lever and the sample surface interfere and local variations of the differences in the two light paths are detected by the photodiode, leading to an intensity offset which additionally depends on the feedback parameters. Because the surface planes of the PP and the PP-*block*-PE are at an angle to each other, horizontal (on PP) and vertical (on PP-*block*-PE) stripes in the LFM image are found. The advantage of the HM-LFM technique is impressively demonstrated in Fig. 8c. The lateral vibration is very small compared with the wavelength of the laser light (630 nm). Because only the high-frequency amplitude is used for data evaluation by the lock-in amplifier, the influence of the interference is cancelled.

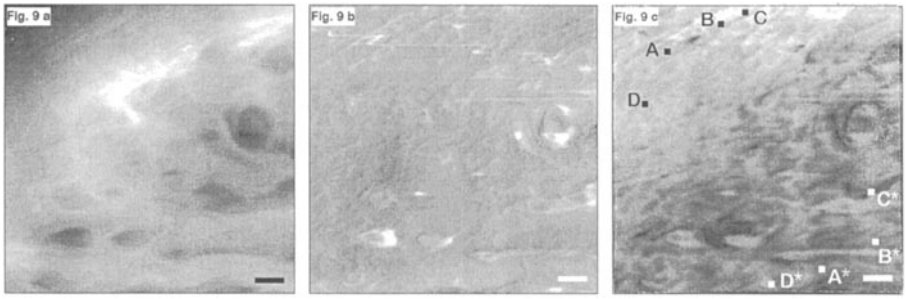

Fig. 9: (a) Topography of sample C (image size 6.9x6.9 μm, bar 700 nm, Δz range 614 nm, scan speed 13 μm/s, normal load $F_N \approx 15$ nN); (b) LFM measured simultaneously; (c) HM-LFM measured simultaneously (lateral vibration < 31 nm, vibration frequency 44 kHz, PP: bright, PP-*block*-PE: dark), the squares mark the end points of the traces given in Fig. 10

This finding encourages to study a medium resolution image of the interface (Fig. 9a). Additionally, the angle between sample surfaces and SFM head was carefully adjusted in the way that the reflected light from the sample surface does not disturb the LFM image. Nevertheless, this procedure does not increase the sensitivity of the LFM method and so the present contrast of micromechanical properties is not visible. Figure 9b is more or less featureless apart from some edge-correlated friction, whereas Fig. 9c clearly demonstrates the superiority of HM-LFM microscopy to the conventional LFM microscopy.

Micromechanical surface properties at the interface of PP and PP-*block*-PE probed with HM-LFM are given in Fig. 10: all four data traces show a smooth transition from PP to PP-*block*-PE crossing the interface region.

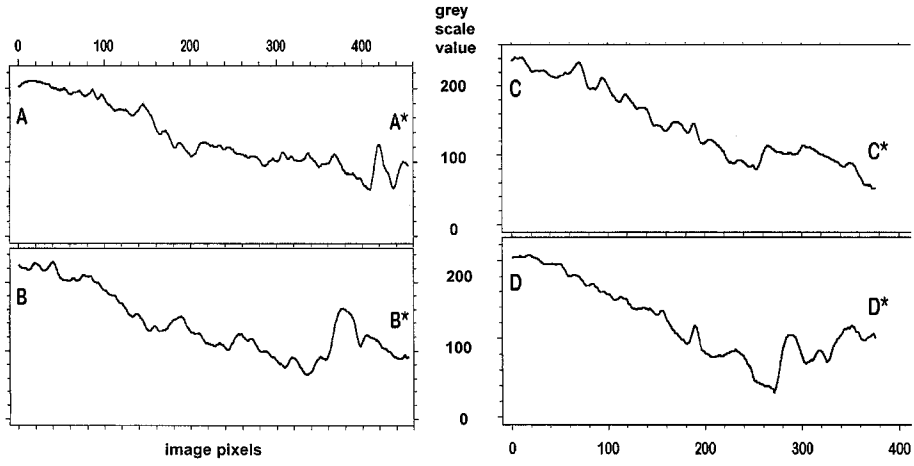

Fig. 10: HM-LFM data during the crossing of the PP/PP-*block*-PE interface

It is reasonable to assume an interface thickness of more than 2 µm, showing the good compatibility between PP and the PP part of the block copolymer. Our experiments with a carbon fiber/poly(phenylene sulfide) interface showed that in this case an interface zone of only 20-80 nm is present[6].

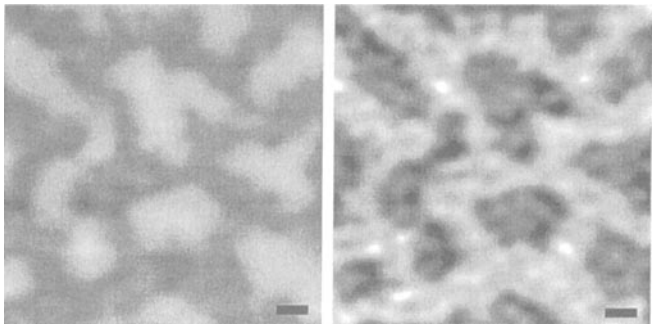

Fig. 11:
Topography (left; bar 60 nm, Δz range 6.3 nm) and HM-LFM contrast (right) of a PS-*block*-PMMA surface (sample D)

First experiments with the surface of a PS/PMMA block copolymer show (Fig. 11), that micromechanical contrasts between the two phases are clearly resolved with HM-LFM[5]. If the lateral vibration is switched off during the scan, no influence on the lateral resolution of the topography is found. Hence, it can be assumed that the lateral vibration amplitude is smaller than 2 nm.

Conclusions

The application of harmonically modulated lateral force microscopy (HM-LFM) is demonstrated with different polymer/polymer interfaces. It can be noted that HM-LFM is a new versatile tool especially for polymer investigation. First of all, its increased sensitivity is worth mentioning. Using low normal forces (< 5 nN) opens a wide range for the examination of micromechanical properties of soft polymer surfaces because the risk of a surface damage decreases. Second important advantage of HM-LFM is that problems with light interference on well reflecting surfaces are suppressed. Third, it is remarkable that friction contrasts on rough surfaces containing information about local micromechanical properties could be achieved without a measurable cross-talk from edge-correlated friction. The experiments show that the stick-slip behaviour of the tip at its point of return in the overscan region can be manipulated with a very small lateral vibration. It can be assumed that the plastic deformation of the polymer surface decreases. This can be useful even in the case that the HM-LFM signal is not measured to reduce mechanical degradation of the polymer surface and contamination of the tip.

Acknowledgements

The authors gratefully acknowledge the financial support from the DFG foundation within the research project A1 of the Sfb 605 'Elementary Friction Processes'. The authors like to thank R. Sernow for technical assistance. Their thanks also due to U. Niebergall, BAM, for valuable discussion about the PP-*block*-PE samples. The cooperation of E. Schadoffsky, TU Clausthal, who prepared the PS-*block*-PMMA copolymer surface, is gratefully acknowledged.

References

1) C. M. Mate, G. M. McClelland, R. Erlandsson, S. Chiang, *Phys. Rev. Lett.* **59**, 1942 (1987)
2) R. Lüthi, E. Meyer, H. Haefke, L. Howald, W. Gutmannsbauer, M. Guggisberg, M. Bammerlin, H.-J. Güntherodt, *Surf. Sci.* **338**, 247 (1995)
3) J. Colchero, *Appl. Phys. Lett.* **68**, 2896 (1996); T. Göddenhenrich, S. Müller, C. Heiden. *Rev. Sci. Instrum.* **65**, 2870 (1994)
4) H. Sturm, W. Stark, E. Schulz, Ger. Patent 195 32 838 (28.8.1995)
5) E. Schadoffsky, H. Sturm, M. Munz, J. Fuhrmann, *2nd Int. Workshop on Wetting and Self-Organisation in Thin Liquid Films*, 2-6.3.1998, poster presentation, Abstracts, p. 62
6) M. Munz, H. Sturm, E. Schulz, G. Hinrichsen, *Composites A* **29**, 1251 (1998)